Diagnostic and Interventional Imaging 102 (2021) 641–648

Original article/*Research, New developments & Artificial Intelligence*

Reduced nontarget embolization and increased targeted delivery with a reflux-control microcatheter in a swine model

Silvia Rizzitelli[a,1,*], Nir Holtzman[b,1], Geert Maleux[c], Thierry De Baere[d], Fei Sun[e], Pierre-Olivier Comby[f], Michael Tal[g], Gwenaelle Bazin[a], Francois Montestruc[h], Thomas Viel[i], Philippe Robert[a], Osnat Harbater[b], Eran Miller[b], Claire Corot[a]

[a] *R&I, Guerbet, 95943 Roissy CdG Cedex, France*
[b] *Guerbet Company, Accurate Medical Therapeutics LTD, 7670203 Rehovot, Israel*
[c] *Radiology, University Hospitals Leuven, 3000 Leuven, Belgium*
[d] *Interventional Radiology, Institut Gustave Roussy, 94800 Villejuif, France*
[e] *Endoluminal Therapy and Diagnosis Unit, Jesús Usón Minimally Invasive Surgery Centre, 10071 Cáceres, Spain*
[f] *Department of Neuroradiology, François-Mitterrand University Hospital, 21079 Dijon, France*
[g] *Interventional Radiology, Hadassah Hospital, 9112001 Jerusalem, Israel*
[h] *MSC, eXYSTAT, 92240 Malakoff, France*
[i] *Life Imaging Facility (PIV), Université de Paris, PARCC-INSERM U970, 75015 Paris, France*

ARTICLE INFO

Keywords:
Embolization, Therapeutic
Interventional radiology
Non-target embolization
X-ray microtomography
Preclinical evaluation

ABSTRACT

Purpose: To evaluate the potential differences in non-target embolization and vessel microsphere filling of a reflux-control microcatheter (RCM) compared to a standard end-hole microcatheter (SEHM) in a swine model.

Materials and methods: Radiopaque microspheres were injected with both RCM and SEHM (2.4-Fr and 2.7-Fr) in the kidneys of a preclinical swine model. Transarterial renal embolization procedures with RCM or SEHM were performed in both kidneys of 14 pigs. Renal arteries were selectively embolized with an automated injection protocol of radio-opaque microspheres. Ex-vivo X-ray microtomography images of the kidneys were utilized to evaluate the embolization by quantification of the deposition of injected microspheres in the target vs. the non-target area of injection. X-ray microtomography images were blindly analyzed by five interventional radiologists. The degree of vessel filling and the non-target embolization were quantified using a scale from 1 to 5 for each parameter. An analysis of variance was used to compare the paired scores.

Results: Total volumes of radio-opaque microspheres injected were similar for RCM (11.5 ± 3.6 [SD] mL; range: 6–17 mL) and SEHM (10.6 ± 5.2 [SD] mL; range: 4–19 mL) (P = 0.38). The voxels enhanced ratio in the target (T) *vs.* non-target (NT) areas was greater with RCM (T = 98.3% *vs.* NT = 1.7%) than with SEHM (T = 89% *vs.* NT = 11%) but the difference was not significant (P = 0.30). The total score blindly given by the five interventional radiologists was significantly different between RCM (12.3 ± 2.1 [SD]; range: 6–15) and the standard catheter (11.3 ± 2.5 [SD]; range: 4–15) (P = 0.0073), with a significant decrease of non-target embolization for RCM (3.8 ± 1.3 [SD]; range: 3.5–4.2) compared to SEHM (3.2 ± 1.5 [SD]; range: 2.9–3.5) (P = 0.014).

Conclusion: In an animal model, RCM microcatheters reduce the risk of non-target embolization from 11% to 1.7%, increasing the delivery of microspheres of 98% to the target vessels, compared to SEHM microcatheters.

Abbreviations: CI, Confidence interval; LS means, Least-squares means; μCT, X-ray microtomography; NTE, Non-target embolization; RCM, Reflux-control micro-catheter; SEHM, Standard end-hole micro-catheter; SD, Standard deviation; TACE, Transcatheter arterial chemoembolization.

* Corresponding author at: R&I, Guerbet, 95943 Roissy CdG Cedex, France.
E-mail address: silvia.rizzitelli@guerbet.com (S. Rizzitelli).

[1] The two authors equally contributed to the research.

https://doi.org/10.1016/j.diii.2021.05.002

1. Introduction

Transcatheter embolization is one of the hallmarks of interventional radiology and widely performed in different pathologies including cancer (mainly hepatocellular carcinoma, renal and lung tumors), uterine leiomyoma, benign prostatic hyperplasia, hemorrhage and vascular anomalies [1]. Technological advances are progressing rapidly in the field of interventional radiology to allow improvement of the performances and a better patient care [2–8].

One of the basic tenets of transcatheter arterial embolization is the controlled delivery of the embolic material to the desired target vessel, minimizing the delivery to the non-targeted tissues [6]. The non-target embolization (NTE) is considered as one of the most important factors leading to complications [9–12]. Such iatrogenesis include inadvertent ischemia of non-targeted tissues, toxicity linked to the drug delivery in the healthy tissues in case drug eluting beads administration or toxicity due to the beta emissions during transarterial radioembolization procedures [10,13–18].

Lung, stomach, pancreas, gallbladder, duodenum, diaphragm, and spleen are the most affected organs by NTE after transcatheter arterial chemoembolization (TACE) [19–25]. Less recurrent but nevertheless dangerous complications include the damages related to transcatheter procedures including uterine fibroid embolization, prostate artery embolization, which affects the rectum, bladder, and penis, and finally bronchial artery embolization for hemoptysis [26–36].

The use of a reflux control device, such as an embolization microcatheter designed to prevent microspheres reflux during embolization appears as an effective means for limiting the risk of NTE and its associated complications. Although several anti-reflux techniques have been developed, they may present drawbacks in routine practice [37–43].

The SeQure® microcatheter, a reflux control microcatheter (RCM) has been designed to locally produce a fluid barrier based on flow dynamics to deliver more microspheres to targeted vessel associated with a decreased risk of NTE. The presence of small slits at the distal end of the microcatheter allows the outflow of the microspheres suspension fluid during their administration, creating thus a fluidic barrier that prevents the back passage of the embolization microspheres along the catheter, thus reducing their reflux (Fig. 1). All the while maintaining the delivery characteristics of a simple end-hole catheter.

The purpose of this study was to evaluate the potential differences in non-target embolization and vessel microsphere filling of a RCM compared to a SEHM in a swine model.

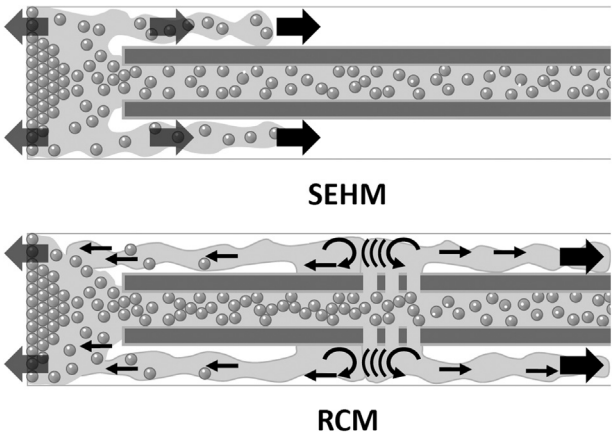

Fig. 1. Drawing illustrates embolic microspheres reflux in standard end-hole microcatheter (SEHM, Top) vs. microspheres reflux with the use of a reflux control microcatheter (RCM, bottom). The presence of lateral slits creates a radial flow of contrast medium allowing a fluidic barrier.

2. Materials and methods

2.1. Animal model

All animal experiments were conducted in compliance with the European Union Directives 2010/63/EU on the protection of animals used for scientific purposes. The protocol was approved by the local animal experiment ethics committees.

Fourteen healthy female landrace domestic pigs (C. Lebeau, Gambais, France) weighing 40–60 kg and 14–21 week-old, were sedated with intramuscular tiletamine 50 mg/mL zolazepam 50 mg/mL (Zoletil® 100, Virbac, 0.055 mL/kg) and xylazine (Xyl-M®, VMD) (2.4 mg/kg, intramuscular), anesthetized using 2% isoflurane (Zoetis), intubated and mechanically ventilated. Animal monitoring was performed continuously during the procedure to determine the depth of anesthesia and physiological status. Heart rate, respiratory rate, body temperature, electrocardiogram, tidal volume and percent inhalant anesthetic administered were continuously monitored and documented every 15–30 min on the procedural data form throughout the procedure.

2.2. In vivo embolization procedure

Embolization procedures were performed using RCM microcatheters (SeQure® 2.4 Fr and 2.7 Fr, Accurate Medical Therapeutics, Guerbet) or SEHM microcatheter (Progreat®, Terumo Interventional Systems) of the same diameter. Radiopaque microspheres (Guerbet Research) with a caliber of 75–150 μm suspended in a solution 0.9% NaCl/iobitridol (Xenetix® 300 mgI/mL, Guerbet) 50:50 were administered for post-procedure visualization.

Twenty-eight swine kidneys were partially embolized (14 kidneys with a 2.4-Fr catheter and 14 kidneys with a 2.7-Fr catheter) with the microspheres by positioning the microcatheter either in the inferior or superior renal arteries under X-ray fluoroscopic imaging (Siemens Siremobil compact L or Philips Veradius). The kidney pole was chosen arbitrarily assuring that the target vessel have no vessels overlap and ensuring the area of interest is supplied by a single vessel. Angiogram of the whole kidney was first performed using a diagnostic 5-Fr catheter (Bern, Imager® II, Boston Scientific) to map the kidney anatomy and identify the target area of injection. The RCM (2.4-Fr or 2.7-Fr) was positioned in the target vessel so that the last slit of the RCM was located 1 cm distal to the bifurcation. Subsequently, one mL of 2 wt% Evans blue dye (Sigma-Aldrich) was locally administered one minute before the mixture associating microspheres and saline/iobitridol (as described above), to target the selected vessels (Fig. 2). The injection of the radiopaque microspheres suspension was performed through an automatic power injector in order to standardize the injection, using a 10 mL syringe, at a flow rate of 8 mL/min, with 7.5 s of injection followed by 30 s of pause. The microspheres suspension was systematically mixed before each injection to ensure a homogeneous suspension. The endpoint criterion was the second observed contrast backflow in non-targeted vessels in order to confirm and validate the complete embolization of the target area.

After embolization of the first kidney, the other kidney of each pig went through the same protocol but with the SEHM replacing the RCM and positioned at the same distance from the vessel bifurcation for comparison purpose. The order of kidney embolization and of the microcatheter used first was randomized.

Upon completion of the procedure, the bladder was emptied using a Foley catheter, and the animals were perfused with saline for one hour after the procedure, to wash out all the contrast medium from the kidneys and avoid contrast artifacts in post-processing images. The animals were euthanized by bolus intravenous of sodium pentobarbital (Dolethal®, Vetoquinol) (182 mg/kg) while under general anesthesia, and the kidneys were

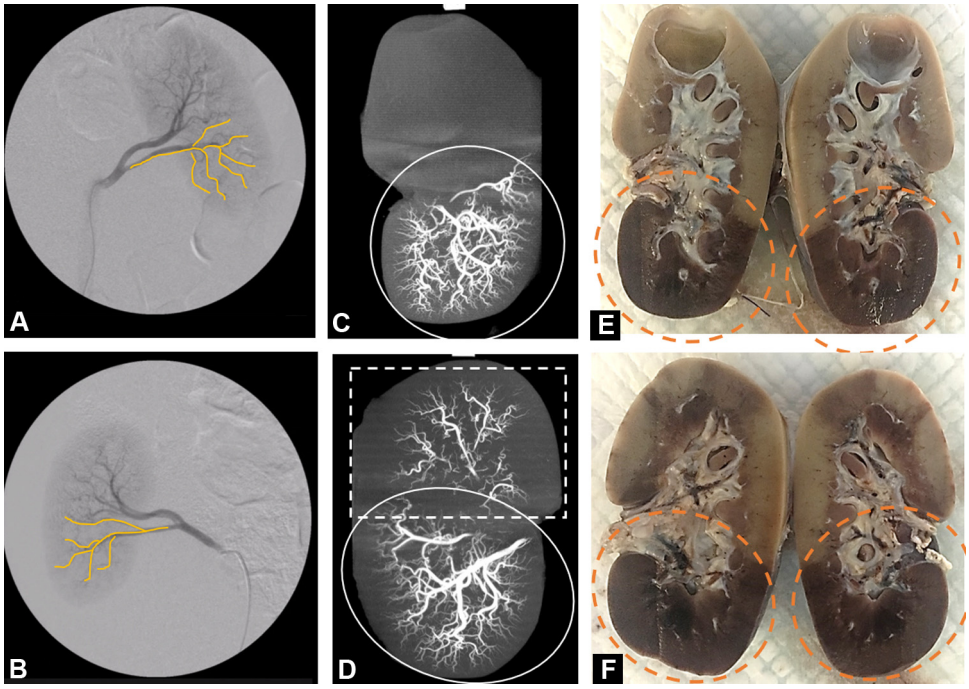

Fig. 2. A, B, Angiograms of the left (A) and right (B) swine kidneys before injection of microspheres. The left kidney (A) was injected using a 2.4-Fr reflux-control micro-catheter and the right kidney (B) using a 2.4-Fr standard end-hole catheter. The yellow line corresponds to the target areas of microspheres injection. C, D, X-ray microtomography projection of the left (C) and right (D) kidneys. The circles correspond to the target area of injection, the rectangles correspond to the non-target area of microspheres injection. E, F, Ex vivo coronal section of the left (E) and right (F) kidneys after embolization. The orange circles correspond to the target areas in injection marked with Evans blue dye.

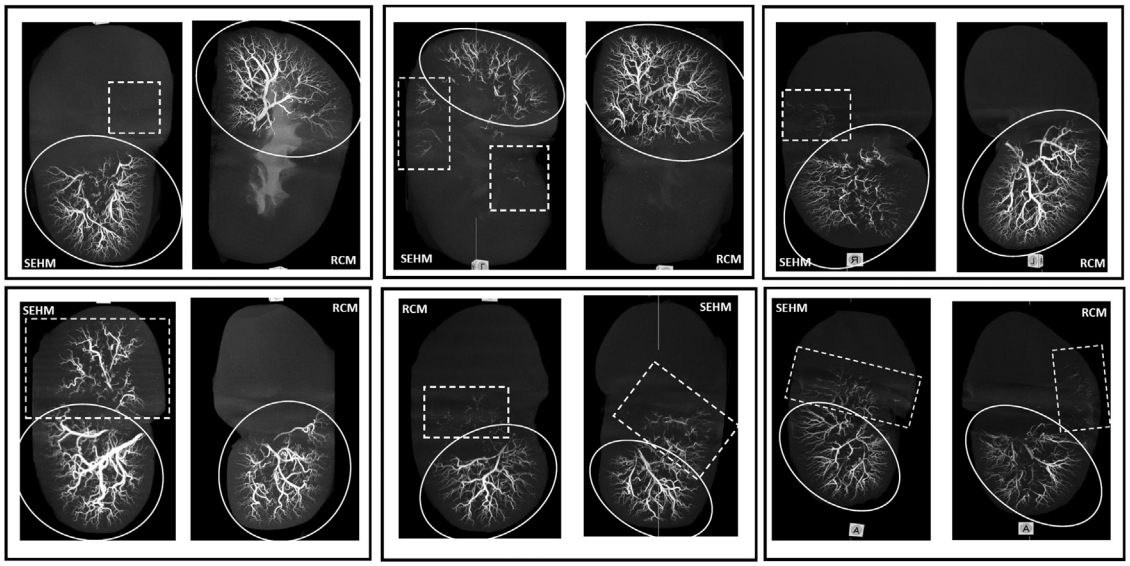

Fig. 3. Ex vivo X-ray microtomography image in three-dimensional projection of the embolized kidneys. For each pair of kidneys, one has been embolized using reflux-control micro-catheter (RCM) and the other using a standard end-hole catheter (SEHM). The circles correspond to the target area of injection, the rectangles correspond to the non-target area of microspheres injection.

harvested to perform X-ray microtomography (μCT) examination for a qualitative evaluation of the intravascular microspheres' distribution (Fig. 3). Moreover, the kidneys were fixed in formaldehyde 0.4% and then cut in coronal sections to detect the Evans blue dye and compare the microspheres localization identified by μCT and the target area. The overlapping of the fluoroscopic angiography and the blue Evans mark determined the identification of the target area of injection. The non-target embolization has been calculated with the presence of μCT contrast enhancement in the areas outside of the target areas due to the presence of the radiopaque microspheres (Fig. 2).

All the analyses were performed on 13 pigs (over 14). One pig was excluded from analyses due to its abnormal renal vascular anatomy not allowing isolating a single area of interest.

2.3. CT imaging

The 26 harvested kidneys were scanned using the preclinical PET-CT NanoScan® camera (Mediso Medical Imaging Systems) with the following parameters: maximum field of view (distance object scanned-X-ray tube: 289 mm)/semi-circular motion/360°/720 projections/70 kV/exposure time: 300 ms per projection/binning 1:1.

The CT projections of the kidneys were reconstructed by filtered back projection using Nucline (v3.00.010.0000) software (Mediso Medical Imaging Systems) as follows: filter: Cosine; cutoff: 100%; size of the voxels: $125 \times 125 \times 125$ μm. μCT images were analyzed with InterView Fusion® software (Mediso Medical Imaging Systems) and processed with Matlab® (The Mathworks Inc.) to quantify the embolization parameters.

For each embolization three parameters were extracted and compared. They included: (*i*), the injected volume of microsphere; (*ii*), the number of enhanced voxels (number of voxels filled by radiopaque microspheres); and (*iii*), the number of nodes (number of bifurcations enhanced correlated to the distality of the embolization). The number of enhanced voxels and the number of nodes were calculated through the μCT analysis.

2.4. Blinded semi-quantitative analysis

The 26 μCT images of the embolized kidneys with the corresponding fluoroscopic images were semi-quantitatively and independently analyzed by five blinded and experienced interventional radiologists (T.D., with 25 years of experience; F.S., with 32 years of experience; G.M., with 23 years of experience; P.C., with 9 years of experience; and M.T., with 20 years of experience). For each blind combination of images, the readers were asked to define a score between 1 and 5, where 1 = "very poor result", 2 = "poor result", 3 = "average result", 4 = "good result" and 5 = "very good result". The readers were asked to quote: (*i*), vessel filling (whether the target vessels were filled by radiopaque microspheres); (*ii*), amount of non-target embolization; and (*iii*), distality of the microspheres accumulation (whether the microspheres are located distally in the micro-vessels and able to deeply embolize the target area).

2.5. Statistical analysis for blinded semi-quantitative analysis

The required sample size of the study was determined based on the following considerations: the null hypothesis to be tested was that score means of both groups were equal. The mean difference to be detected was 1 point with an equal standard deviation for both groups of 2 points. Therefore, a sample size of 64 observations per catheter achieves 80% power to reject the null hypothesis. Significance level (alpha) was set at 5% using a two-sided two-sample equal-variance Student *t* test. Considering a 10% missing data rate, a sample size of 70 observations per catheter was considered sufficient for this blinded semi-quantitative analysis. This sample size was achieved by including 13 swines for 5 readers and 2 locations, leading to 130 expected values for each score (65 per catheter). Each of the three scores (/5) and the total score (/15) was described using means and standard deviations and medians with intra-quartile range.

Analyses were conducted using SAS v9.4; all reported *P* values were two-sided and considered statistically significant when less than 5%. Inferential analyses used a general linear model with reader and catheter (SEHM/RCM) as factors. Interactions were explored. Estimates of least-squares means (LSmeans) and 95% confidence intervals (CI) were generated. As sensitivity analysis, each of the three scores was categorized in three classes: 1–2, 3–4 and 5 and 1–5, 5–10, 10–15 for the total score. Categorical variables were expressed as proportions and percentages and differences in categories were tested using Fisher exact test and logistic regressions with the same model with reader and catheter.

3. Results

3.1. In vivo experiments

The volumes of radiopaque microspheres injected until reaching embolization endpoint with RCM (11.2 ± 3.6 [SD] mL; range: 6–17 mL) and SEHM (10.6 ± 5.2 [SD] mL; range: 4–19 mL) did not significantly differ ($P = 0.38$). At μCT analysis, the number of enhanced voxels at the target area using RCM (453 ± 156 [SD]; range: 168–725) was not significantly different from that measured with SEHM (395 ± 209 [SD]; range: 107–835) ($P = 0.31$). The number of enhanced voxels measured in the non-target area using SEHM (42.8 ± 95.7 [SD]; range: 0–345) was not significantly different from that using RCM (7.6 ± 17.6 [SD] range: 0–65) ($P = 0.21$) despite a high variability (Fig. 3).

Although a similar volume of microspheres was administered with both microcatheters, RCM delivered a proportion of 98% of microspheres into the target site while the SEHM delivered 89% of microspheres into the target site, but the difference was not significant ($P = 0.30$) and, therefore, 11% of microspheres corresponded to NTE in the latter case *vs.* 2% with RCM (Figs. 4 and 5).

3.2. Blinded semi-quantitative analysis

A significant difference in the total scores was observed between RCM and the standard catheter ($P = 0.0041$) in the analysis of variance model with an LSMeans of 11.6 (95% CI: 11.0–12.2) *vs.* 10.3 (95% CI: 9.8–10.9), respectively and an LSMeans difference of −1.2 (95% CI: −2.1– −0.40). Reader effect was also observed with a total score from 10.0 (95% CI: 9.1–10.9) for E to 12.1 (95% CI: 11.2–13.0) for B ($P = 0.01$). No interaction catheter-reader was observed ($P = 0.98$).

A significant difference in non-target embolization was observed between RCM and the standard catheter ($P = 0.0141$) with LSMeans of 3.8 (95% CI: 3.5–4.2) *vs.* 3.2 (95% CI: 2.9–3.5), respectively; and an LSMeans difference of −0.6 (95% CI: −1.1– −0.10). No reader effect was observed ($P = 0.01$).

Differences were not statistically significant for vessel filling (4.1 [95% CI: 3.9–4.3] for RCM *vs.* 3.9 [95% CI: 3.7–4.1] for SEHM) ($P = 0.13$) or distality (4.4 [95% CI: 4.2–4.5] for RCM *vs.* 4.2 [95% CI: 4.0–4.3] for SEHM) ($P = 0.12$) with a strong reader effect for both ($P < 0.001$) without interaction (Table 1).

A significant 20% difference was observed for the number of observations with a total score between 10 and 15 with 82% (53/65) observations for RCM *vs.* 62% (40/65) for the SEHM ($P = 0.017$). Significant difference was observed for non-target embolization with 42% (27/65) of observations with a score of 5 for RCM *vs.* 29% (19/65) for the SEHM ($P = 0.032$). The difference was not statistically significant for filling with percentages of 39% (25/65) with a score of 5 for RCM *vs.* 35% (23/65) for SEHM ($P = 0.48$) or distality with percentages of 51% (33/65) for RCM *vs.* 42% (27/65) for SEHM ($P = 0.11$). Differences between readers were also observed and were only significant for filling and distality but not for the total score or non-target embolization (Fig. 6).

4. Discussion

During embolization with microspheres, while the ability to locally administer specific microsphere volumes can be affected by the physicochemical characteristics of the microspheres and by the suspension quality [2], it also strongly depends on the characteristics of the delivery microcatheter as well as the treatment selectivity and the vascular anatomy. In case of reflux, underdosing or non-target embolization can result in reduced efficacy and/or increased side effects [10,44]. In addition to navigability, a success-

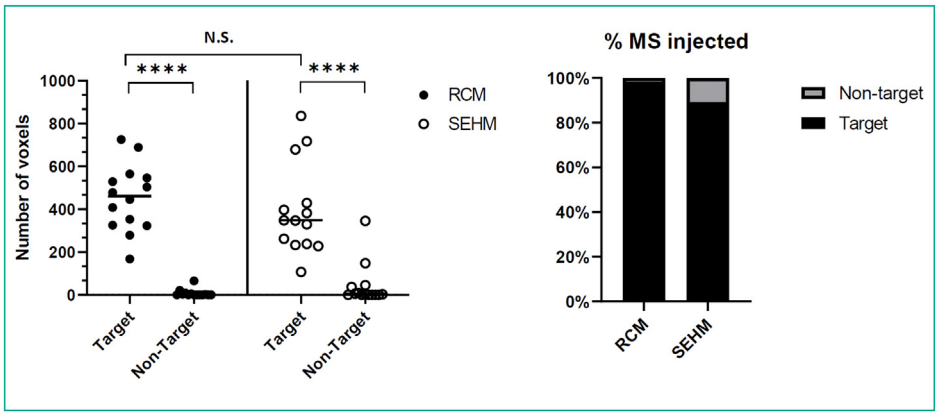

Fig. 4. Quantification of contrast enhancement on X-ray microtomography in the swine kidneys of the target vs. non-target areas of injection. The difference between the target vs. the non-target areas is statistically significant for the two catheters (****), while the difference between reflux-control micro-catheter (RCM) and the standard end-hole micro-catheter (SEHM) is not significant (N.S.).

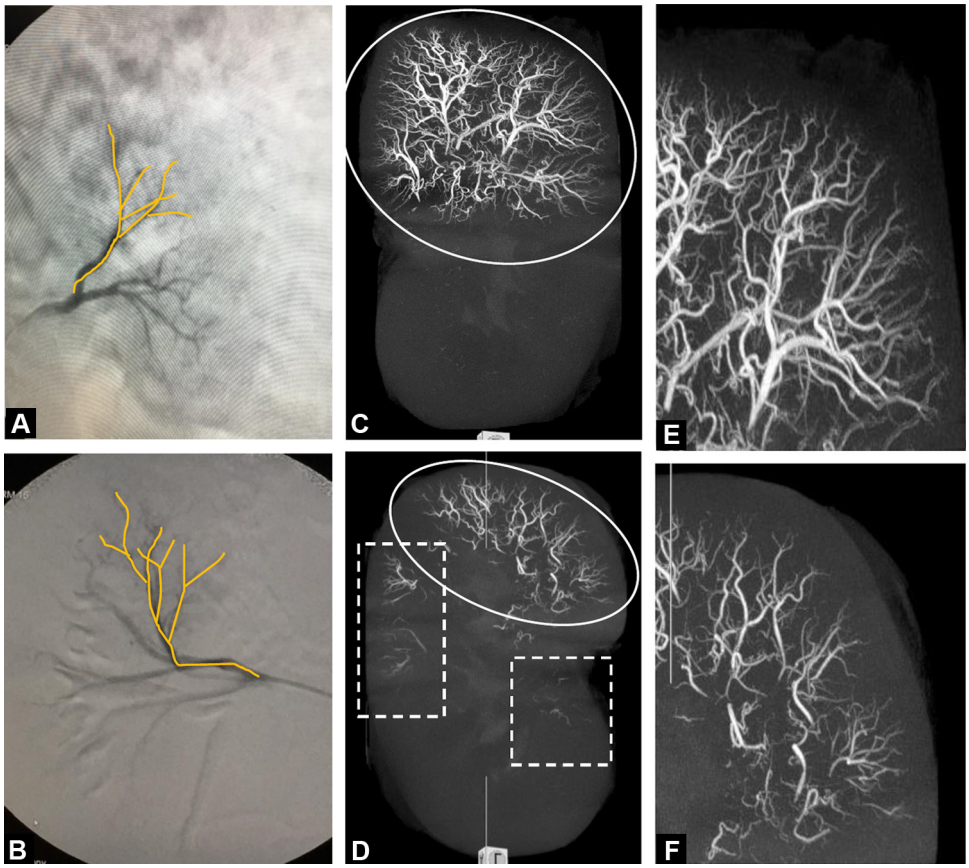

Fig. 5. A, B, Angiogram of the left (A) and right (B) kidneys before injection of microspheres. The left (A) kidney was injected using a 2.4-Fr reflux-control micro-catheter, the right (B) kidney using a standard end-hole catheter. C, D, X-ray microtomography projection of the left (C) and right (D) kidneys. The circles correspond to the target area of injection, the rectangles correspond to the non-target area of microspheres injection. E, F, Magnified X-ray microtomography projection images show distal renal parenchyma of the left (E) and right (F) kidneys.

ful embolization often requires a slow injection rate to reduce the risk of reflux.

The presence of slits at the distal section of the RCM micro-catheter was designed to (*i*), visualize, under fluoroscopy, the radial flow of iodinated contrast medium exiting from the distal end of the catheter, thus providing an indication on the vessel flow dynamics; (*ii*), to reduce the embolic material velocity and its flow rate in the distal end of the microcatheter section because of the flow splitting between the distal and radial flows; and (*iii*), to create an external "fluidic barrier" around the distal end of the catheter, due to the combination of (*i*) and (*ii*). This barrier aims at enabling reflux-controlled delivery of embolization microspheres at much higher injection rates than possible using standard microcatheters. Therefore, this approach should facilitate the injection of a higher amount of embolic material until full stasis is achieved in the target area, using a normal injection flow rate.

This study using a swine model was undertaken with the aims of evaluating the microspheres embolization effect on healthy tissues with RCM versus the same SEHM, and visualizing the amount of microspheres delivered in the target versus non-target sites

Table 1
Least square means and 95% confidence interval per reader and overall. Analysis of variance model with catheter, reader and reader per catheter interaction.

	Filling		Anti-reflux		Distality		Total score	
	RCM	SEHM	RCM	SEHM	RCM	SEHM	RCM	SEHM
T.D.	3.4 (2.9; 3.9)	3.2 (2.7; 3.6)	4.2 (3.4; 5.0)	3.3 (2.5; 4.1)	3.8 (3.4; 4.2)	3.6 (3.2; 4.0)	11.0 (9.6; 12.3)	9.4 (8.1; 10.8)
F.S.	4.8 (4.3; 5.2)	4.5 (4.1; 5.0)	3.7 (2.9; 4.5)	2.9 (2.1; 3.7)	5.0 (4.6; 5.0)	4.8 (4.4; 5.0)	12.5 (11.2; 13.8)	11.7 (10.4; 13.1)
G.M.	4.3 (3.8; 4.8)	4.2 (3.7; 4.6)	3.8 (3.1; 4.6)	3.5 (2.8; 4.3)	4.3 (3.9; 4.7)	4.2 (3.8; 4.6)	11.7 (10.4; 13.1)	10.6 (9.2; 11.9)
P.C.	4.4 (3.9; 4.9)	4.0 (3.5; 4.5)	3.9 (3.1; 4.7)	3.4 (2.6; 4.2)	4.5 (4.1; 4.9)	4.3 (4.1; 4.9)	12.1 (10.8; 13.5)	10.6 (9.2; 11.9)
M.T.	3.8 (3.3; 4.2)	3.6 (3.1; 4.1)	3.4 (2.6; 4.2)	2.8 (2.1; 3.6)	4.2 (3.8; 4.6)	3.9 (3.5; 4.3)	10.6 (9.2; 11.9)	9.4 (8.1; 10.8)
Overall	4.1 (3.9; 4.3)	3.9 (3.7; 4.1)	3.8 (3.5; 4.2)	3.2 (2.9; 3.5)	4.4 (4.2; 4.5)	4.2 (4.0; 4.3)	11.6 (11.0; 12.2)	10.3 (9.7; 10.9)

Numbers in parentheses are 95% confidence interval. RCM: Reflux control microcatheter; SEHM: Standard end-hole microcatheter; T.D., F.S., G.M., P.C., M.T.: Interventional radiologists involved in the reading.

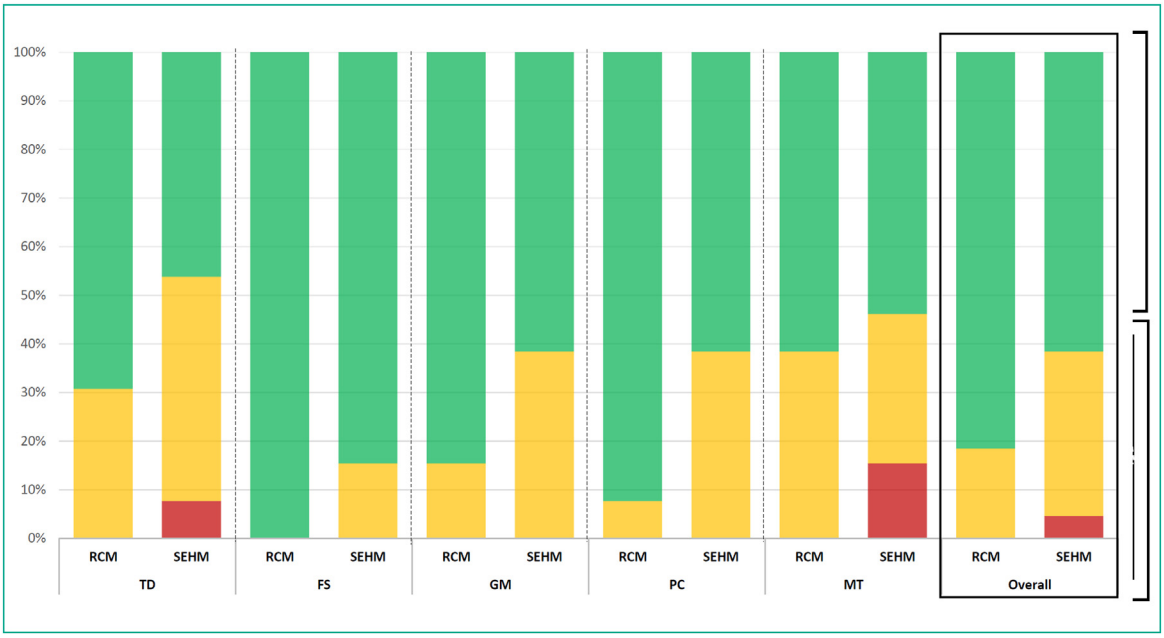

Fig. 6. Diagram shows percentage of the total scoring for all the kidneys analyzed by five readers.

through imaging techniques. Because of its high resolution, the μCT technique allows an accurate analysis of the distribution of the radiopaque microspheres into non-target vessels [9,45].

The swine model is an appropriate model to test the delivery, positioning and deployment of the studied device as the porcine cardiovascular anatomy is considered a relevant and the closest *in vivo* model that reliably mimics human vascular anatomy of pathologies such as tumors and is widely used for such applications [46]. The use of an automatic injector for the microspheres administration allowed the standardization of the injection flow rate without the need to reduce the flow rate during the procedure. The visualization of the radial flow of iodinated contrast medium exiting through the slits of RCM was the key criterion for defining the end of the injection.

The μCT analysis demonstrated that the number of enhanced voxels in the target area was higher for RCM than with its comparator standard end-hole microcatheter, while a greater number of microspheres was measured in the non-target area for the SEHM than with RCM. Even if these results are not statistically significant, this result might have an important clinical relevance, significantly reducing the damages caused by NTE.

From a qualitative point of view, RCM was able to achieve a better filling of the target blood vessels inducing a more effective embolization compared to the SEHM. Similarly, RCM showed a better reflux control for non-target embolization than SEHM, thus potentially leading to less adverse effects. From a quantitative point of view, for the same volume of microspheres injected, RCM helped deliver a greater amount of microspheres in the target area with a lower NTE than SEHM.

The qualitative observation of the μCT images of the kidneys embolized with the radiopaque microspheres, performed by five blinded interventional radiologists, demonstrates an overall superiority of RCM compared to SEHM. The vessels appeared bright in distality (microvasculature) as well as the main vascular branches, with less interruption than those injected with the control SEHM for the blind readers. This means that injecting with a RCM allows reaching a better filling of the kidney vessels than with the control end-hole catheter, and that the resulting embolization tended to be more effective than the one induced by the standard microcatheter used for comparison. Therefore, all the observers considered that the presence of NTE was statistically greater for the SEHM than for RCM, confirming the activity of reflux control of the microcatheter.

This study has some limitations. All the preclinical experiments presented here were carried out with an automatic injector for standardization purpose, which is not representative of the clinical practice. The flow rate used for those in vivo experiments was useful to standardize the injection, but do not necessarily uniformly represent common clinical practice. Moreover, pig vascular anatomy shows a high variability among animals. Further investigations including the therapeutic efficacy of RCM on a more translational pathological model are planned.

In conclusion, this study illustrates that the fluid barrier created by the RCM has a tendency to deliver a greater amount of microspheres to the target area of injection compared to SEHM, in addition of demonstrating less NTE. This study paves the way to further clinical studies with the aim of investigating the clinical consequences of these findings.

Human rights

The authors declare that the work described has been carried out in accordance with the EU Directive 2010/63/EU for animal experiments.

Informed consent and patient details

The authors declare that the work described does not involve patients or volunteers.

Funding

This work did not receive any grant from funding agencies in the public, commercial, or not-for-profit sectors.

Author contributions

All authors attest that they meet the current International Committee of Medical Journal Editors (ICMJE) criteria for Authorship.

Acknowledgments

The authors thank: JM. Idée, X. Violas, W. Gonzalez, C. Robic, D. Balvay, B. Tavitian, T. Shalem, K. Shtiegman, M. Lemaître, T. Dagan, A. Seron, Y. Zipory, B. Piednoir and M. Soares for their contribution to this study.

Disclosure of interest

The authors declare that they have no competing interest.

References

[1] Wang YX, De Baere T, Idée JM, Ballet S. Transcatheter embolization therapy in liver cancer: an update of clinical evidences. Chin J Cancer Res 2015;27:96–121.
[2] Hu J, Albadawi H, Chong BW, Deipolyi AR, Sheth RA, Khademhosseini A, et al. Advances in biomaterials and technologies for vascular embolization. Advance Mat 2019;31:e1901071.
[3] Leyon JJ, Littlehales T, Rangarajan B, Hoey ET, Ganeshan A. Endovascular embolization: review of currently available embolization agents. Curr Probl Diagn Radiol 2014;43:35–53.
[4] Vaidya S, Tozer KR, Chen J. An overview of embolic agents. Semin Intervent Radiol 2008;25:204–15.
[5] Venturini M, Lanza C, Marra P, Colarieti A, Panzeri M, Augello L, et al. Transcatheter embolization with Squid, combined with other embolic agents or alone, in different abdominal diseases: a single-center experience in 30 patients. Cardiovasc Intervent Radiol 2019;2:8.
[6] Diop AD, Diop AN, Hak JF, Di Bisceglie M, Bartoli JM, Guillet B, et al. Hemostatic embolization of renal artery pseudoaneurysm using absorbable surgical suture (FairEmbo concept). Diagn Interv Imaging 2020;101:757–8.
[7] Iguchi T, Hiraki T, Matsui Y, Fujiwara H, Sakurai J, Baba K, et al. Embolization using hydrogel-coated coils for pulmonary arteriovenous malformations. Diagn Interv Imaging 2020;101:129–35.
[8] Virdis F, Reccia I, Di Saverio S, Tugnoli G, Kwan SH, Kumar J, et al. Clinical outcomes of primary arterial embolization in severe hepatic trauma: a systematic review. Diagn Interv Imaging 2019;100:65–75.
[9] Arepally A, Chomas J, Kraitchman D, Hong K. Quantification and reduction of reflux during embolotherapy using an antireflux catheter and tantalum microspheres: ex vivo analysis. J Vasc Interv Radiol 2013;24:575–80.
[10] López-Benítez R, Richter GM, Kauczor HU, Stampfl S, Kladeck J, Radeleff BA, et al. Analysis of nontarget embolization mechanisms during embolization and chemoembolization procedures. Cardiovasc Intervent Radiol 2009;32:615–22.
[11] Malagari K, Pomoni M, Spyridopoulos TN, Moschouris H, Kelekis A, Dourakis S, et al. Safety profile of sequential transcatheter chemoembolization with DC Bead™: results of 237 hepatocellular carcinoma (HCC) patients. Cardiovasc Intervent Radiol 2011;34:774–85.
[12] Ramirez M, Ravichandran S, Ronald L, Pabon-Ramos WM, Smith TP, Kim CY, et al. Recognition and management of dermatologic complications from interventional radiology procedures. Diagn Interv Imaging 2019;100:659–70.
[13] Chao C, Stavropoulos SW, Mondschein JI, Dagli M, Sudheendra D, Nadolski G, et al. Effect of substituting 50% Isovue for sterile water as the delivery medium for SIR-spheres: improved dose delivery and decreased incidence of stasis. Clin Nucl Med 2017;42:176–9.
[14] Massmann A, Rodt T, Marquardt S, Seidel R, Thomas K, Wacker F, et al. Transarterial chemoembolization (TACE) for colorectal liver metastases:current status and critical review. Langenbeck Arch Surg 2015;400:641–59.
[15] Smith MT, Johnson DT, Gipson MG. Skin necrosis resulting from nontarget Embolization of the falciform artery during transarterial chemoembolization with drug-eluting beads. Semin Intervent Radiol 2015;32:22–5.
[16] Stampfl U, Bermejo JL, Sommer CM, Hoffmann K, Weiss KH, Schirmacher P, et al. Efficacy and nontarget effects of transarterial chemoembolization in bridging of hepatocellular carcinoma patients to liver transplantation: a histopathologic study. J Vasc Interv Radiol 2014;25, 1018–26.e4.
[17] van Hazel GA, Heinemann V, Sharma NK, Findlay MP, Ricke J, Peeters M, et al. SIRFLOX: randomized phase III trial comparing first-line mFOLFOX6 (plus or minus bevacizumab) versus mFOLFOX6 (plus or minus bevacizumab) plus selective internal radiation therapy in patients with metastatic colorectal cancer. J Clin Oncol 2016;34:1723–31.
[18] Ghosn M, Derbel H, Kharrat R, Oubaya N, Mulé S, Chalaye J, et al. Prediction of overall survival in patients with hepatocellular carcinoma treated with Y-90 radioembolization by imaging response criteria. Diagn Interv Imaging 2021;102:35–44.
[19] Abdel-Rahman O, Elsayed Z. Yttrium-90 microsphere radioembolisation for unresectable hepatocellular carcinoma. Cochrane Database Syst Rev 2020;11:Cd011313.
[20] Ingraham CR, Johnson GE, Nair AV, Padia SA. Nontarget embolization complicating transarterial chemoembolization in a patient with hepatocellular carcinoma. Semin Intervent Radiol 2011;28:202–6.
[21] Malagari K, Pomoni M, Moschouris H, Kelekis A, Charokopakis A, Bouma E, et al. Chemoembolization of hepatocellular carcinoma with HepaSphere 30-60 μm: safety and efficacy study. Cardiovasc Intervent Radiol 2014;37:165–75.
[22] Newgard BJ, Getrajdman GI, Erinjeri JP, Covey AM, Brody LA, Sofocleous CT, et al. Incidence and consequence of nontarget embolization following bland hepatic arterial embolization. Cardiovasc Intervent Radiol 2019;42:1135–41.
[23] Urbano J, Echevarria-Uraga JJ, Ciampi-Dopazo JJ, Sánchez-Corral JA, Cobos Alonso J, Anton-Ladislao A, et al. Multicentre prospective study of drug-eluting bead chemoembolisation safety using tightly calibrated small microspheres in non-resectable hepatocellular carcinoma. Eur J Radiol 2020;126:108966.
[24] Yamaguchi T, Seki T, Komemushi A, Suwa K, Tsuda R, Inokuchi R, et al. Acute necrotizing pancreatitis as a fatal complication following DC Bead transcatheter arterial chemoembolization for hepatocellular carcinoma: a case report and review of the literature. Mol Clin Oncol 2018;9:403–7.
[25] de Baere T, Arai Y, Lencioni R, Geschwind JF, Rilling W, Salem R, et al. Treatment of liver tumors with Lipiodol TACE: technical recommendations from experts opinion. Cardiovasc Intervent Radiol 2016;39:334–43.
[26] Cadour F, Tradi F, Habert P, Scemama U, Vidal V, Jacquier A, et al. Prostatic artery embolization using three-dimensional cone-beam computed tomography. Diagn Interv Imaging 2020;101:721–5.
[27] Fruchter O, Schneer S, Rusanov V, Belenky A, Kramer MR. Bronchial artery embolization for massive hemoptysis: long-term follow-up. Asian Cardiovasc Thorac Ann 2015;23:55–60.
[28] Goldberg J, Pereira L. Pregnancy outcomes following treatment for fibroids: uterine fibroid embolization versus laparoscopic myomectomy. Curr Opin Obstet Gynecol 2006;18:402–6.
[29] Gonsalves C, Franciosa SV, Shah S, Bonn J, Wu C. Patient presentation and management of labial ulceration following uterine artery embolization. Cardiovasc Intervent Radiol 2007;30:1263–6.
[30] Gupta A, Sands M, Chauhan NR. Massive hemoptysis in pulmonary infections: bronchial artery embolization. J Thorac Dis 2018;10:S3458–64.
[31] Isaacson AJ, Piechowiak RL, Nutting C, Bagla S. How to "get out of trouble" during prostatic artery embolization. Tech Vasc Interv Radiol 2018;21:288–94.
[32] Panda A, Bhalla AS, Goyal A. Bronchial artery embolization in hemoptysis: a systematic review. Diagn Interv Radiol 2017;23:307–17.
[33] Payne JF, Robboy SJ, Haney AF. Embolic microspheres within ovarian arterial vasculature after uterine artery embolization. Obstet Gynecol 2002;100:883–6.
[34] Sidhu M, Wieseler K, Burdick TR, Shaw DW. Bronchial artery embolization for hemoptysis. Semin Interv Radiol 2008;25:310–8.
[35] Wang M, Guo L, Duan F, Yuan K, Zhang G, Li K, et al. Prostatic arterial embolization for the treatment of lower urinary tract symptoms as a result of large

benign prostatic hyperplasia: a prospective single-center investigation. Int J Urol 2015;22:766–72.
[36] Cornelis FH, Barral M, Jenoudet H, Boutault JR, Zurlinden O. Successful conservative management of non-targeted embolization of the penile glans after prostate artery embolization. Diagn Interv Imaging 2020;101:617–8.
[37] Lenton J, Kessel D, Watkinson AF. Embolization of renal angiomyolipoma: immediate complications and long-term outcomes. Clin Radiol 2008;63:864–70.
[38] Rose SC, Kikolski SG, Chomas JE. Downstream hepatic arterial blood pressure changes caused by deployment of the surefire antireflux expandable tip. Cardiovasc Intervent Radiol 2013;36:1262–9.
[39] Lucatelli P, De Rubeis G, Rocco B, Basilico F, Cannavale A, Abbatecola A, et al. Balloon occluded TACE (B-TACE) vs. DEM-TACE for HCC: a single center retrospective case control study. BMC Gastroenterol 2021;21:51.
[40] Lucatelli P, Ginnani Corradini L, De Rubeis G, Rocco B, Basilico F, Cannavale A, et al. Balloon-occluded transcatheter arterial chemoembolization (b-TACE) for hepatocellular carcinoma with PEG epirubicin-loaded DEB. Cardiovasc Intervent Radiol 2019;42:853–62.
[41] Sadekni S, Moustafa AS, Moawad S, Mahmoud K, Hamed BF, Abdelal AK. Approaches for safe transarterial chemoembolization of multifocal hepatocellular carcinoma with retrograde flow in a retroportal artery. Radiol Case Rep 2018;13:171–4.
[42] Titan JJ, Fishman AM, Cherian A, Tully M, Stein LL, Jacobs L, et al. End-hole versus microvalve infusion catheters in drug-eluting microspheres-TACE for solitary hepatocellular carcinoma: a retrospective analysis. Cardiovasc Intervent Radiol 2019;42:560–8.
[43] Xu Z, Jernigan S, Kleinstreuer C, Buckner GD. Solid tumor embolotherapy in hepatic arteries with an anti-reflux catheter system. Ann Biomed Eng 2016;44:1036–46.
[44] Aliberti C, Carandina R, Sarti D, Pizzirani E, Ramondo G, Cillo U, et al. Transarterial chemoembolization with DC Bead LUMI™ radiopaque beads for primary liver cancer treatment: preliminary experience. Future Oncol 2017;13:2243–52.
[45] Sharma KV, Dreher MR, Tang Y, Pritchard W, Chiesa OA, Karanian J, et al. Development of "imageable" beads for transcatheter embolotherapy. J Vasc Interv Radiol 2010;21:865–76.
[46] Moreira PL, An YH. Animal models for therapeutic embolization. Cardiovasc Intervent Radiol 2003;26:100–10.